Response to Editor

The authors greatly acknowledge the editor for carefully reading the manuscript and providing constructive comments. This document contains the author's responses.

Editor's comments

Authors response

Changes in the manuscript

Thank you for providing replies to the second round of Referee comments. I understand that you have addressed all their concerns and hope that they are satisfied as well. I am thus happy to accept your work for publication in ACP. However, please take the time to consult the ACP guidelines regarding Abstract and Conclusions before uploading the final version of your manuscript (https://www.atmospheric-chemistry-and-hysics.net/policies/guidelines_for_authors.html)

We have reduced the abstract to approximately 250 words, and now it is given by

This work investigates the scattering matrix elements during different Saharan dust outbreaks over Granada (South-East Spain) in 2022 using a Polarized Imaging Nephelometer (PI-Neph) capable of measuring continuously the phase function (F_{11}) and the polarized phase function ($-F_{12}/F_{11}$) at three different wavelengths (405, 515 and 660 nm) in the range 5° - 175°. The focus is in two extreme dust events (PM_{10} > 1000 μgm^{-3}) in March 2022. During the peaks of these events F_{11} and $-F_{12}/F_{11}$ show the classical patterns observed for dust samples in laboratory measurements available in the Amsterdam-Granada Light Scattering database at all wavelengths. However, for the moments prior and after the peaks the results reveal important sensitivity in $-F_{12}/F_{11}$ at 405 nm. For the other wavelengths, however, this difference in $-F_{12}/F_{11}$ is not evident. Moreover, no remarkable changes are found in F_{11} that is always characterized by strong predominance of forward scattering. The analyses of more frequent and moderate events registered in summer 2022 (PM_{10} between 50 and 100 μgm^{-3}) revealed F_{11} and $-F_{12}/F_{11}$ patterns like those observed prior and after the extreme events. The combination of PI-Neph measurements with additional in-situ instrumentation allowed a typing classification that revealed the peaks in the extreme dust events as pure dust, while for the rest of cases remarked a mixture of dust with urban background pollution. In addition, simulations with the Generalized Retrieval of Atmosphere and Surface Properties (GRASP) code explain the different patterns in $-F_{12}/F_{11}$ with changes in the refractive indexes and with the different contributions of the fine and coarse mode.

Additionally, we have shortened the conclusions section, keeping focus in the most relevant results and findings (Lines 789 - 858)

This work has focused on the analyses of aerosol phase matrix elements and other optical properties during Saharan dust outbreaks that were registered in the UGR station (Southeastern Spain) in the year 2022. The main novelty of the analyses are the measurements by the multiwavelength Polarized Imaging Nephelometer (PI-Neph) developed by GRASP-Earth and capable of providing two aerosol scattering matrix elements (F_{11} and $-F_{12}/F_{11}$) for three different wavelengths (405, 515 and 660 nm). The uniqueness of PI-Neph is that it allows to measure phase matrix elements of ambient aerosol. The optimization of the instrument and the data quality check applied served to obtain (F_{11} and $-F_{12}/F_{11}$) with uncertainties below 10% and 20%, respectively. The multiwavelength F_{11} and $-F_{12}/F_{11}$ measurements for different Saharan dust

outbreaks are some of the first carried out for ambient aerosol and serve to complement laboratory measurements of mineral dust particles and of synthetic samples minerals that compose dust particles. The novel measurements of F_{11} and $-F_{12}/F_{11}$ can also complement other optical and microphysical properties of Saharan dust already known from in-situ instrumentation and by active and passive remote sensing instruments, both from the ground and the space.

The analyses differentiate between two different scenarios: the first is two extreme Saharan dust outbreaks that happened on $15^{th} - 16^{th}$ (peaks in $PM_{10} \sim 1800$ μgm^{-3}) and on $25^{th} - 26^{th}$ March 2022 (peaks in $PM_{10} \sim 690$ μgm^{-3}) when the daily limit value of 50 μgm^{-3} delimited by the 2008/50/CE European Directive was exceeded. The detailed temporal evolution analysis of F_{11} for these extreme events did not show relevant changes with time, showing the classical pattern for predominance of big and non-spherical particles characterized by high predominance of forward scattering and almost negligible wavelength differences. For $-F_{12}/F_{11}$ at 515 and 660 nm there were no remarkable differences with time showing bell-shape pattern centered ~90° and with slightly positive values (maximums ~0.2). However, for 405 nm this bell-shape pattern was present only for the instants of extreme predominance of dust, while for the other instants $-F_{12}/F_{11}$ showed a very different pattern with values close to zero up to 50° - 60° followed by a decrease to values between -0.4 and -0.6 in the region around 120° and a final increase recovering to values close to zero in the backward region. On the other hand, the second analysis scenario was the period April – September 2022 when more moderate Saharan dust intrusions were registered (maximum PM_{10} around 100 μgm^{-3}. F_{11} mostly followed the classical pattern characterized by strong forward scattering, although some cases showed some spectral dependence on 405 nm depending on the influence of fine mode particles in the mixture. However, the analysis of $-F_{12}/F_{11}$ revealed big differences among wavelengths, being 405 nm like the pattern observed during the moments prior and after the peaks of the extreme dust events. The typing classification with additional in-situ measurements classified the peaks of the extreme dust events as pure dust while for the rest of measurements indicated a mixture of dust particles with local anthropogenic pollution, which can be the reason that explain the differences in $-F_{12}/F_{11}$. Thus, polarization at 405 nm seems to be very sensitive to the presence of additional anthropogenic particles in the sample dominated by mineral dust For 515 and 660 nm there are large variability depending on the mixture of particles. Nevertheless, more F_{11} and $-F_{12}/F_{11}$ measurements are needed at other experimental sites to have a more complete vision of mineral dust role on climate.

Laboratory measurements of mineral dust samples available in the Granada-Amsterdam Light Scattering Database provided F_{11} and $-F_{12}/F_{11}$ at 488 and 632 nm, allowing for a comparative assessment. To that end, averages of the period April – September 2022 plus the peaks of the extreme events during March 2022 were used. The results showed that for all normalized F_{11} the differences between temporal averages, peak events and laboratory measurements were minimal, being only notable in the backscattering region close to 180° where according to the T-Matrix theory more sensitive to aerosol particle parameters is found. For $-F_{12}/F_{11}$ laboratory measurements showed a bell-shape pattern with maximums around 0.2 in the region ~ 90º both at 488 and 632 nm, indicating very good agreement with the PI-Neph seasonal averages at 660 nm but important departures when comparing with 405 nm. However, during the peaks of the extreme dust events $-F_{12}/F_{11}$ comparisons with laboratory measurements agree quite well. Considering that laboratory measurements consist of pure dust samples directly collected in the dessert, we can conclude that the $-F_{12}/F_{11}$ at 405 nm measured in the laboratory is only reproduced when there are extreme concentrations of dust in the atmosphere, while the contribution of anthropogenic particles in the mixture the $-F_{12}/F_{11}$ affects critically to $-F_{12}/F_{11}$. For the other channels, particularly 660 nm, $-F_{12}/F_{11}$ seems to be less critically affected by the contribution of anthropogenic particles. We therefore believe that multiwavelength polarized polar nephelometry opens new possibilities in the studies of mineral dust role in the climate system.

Simulations performed by the GRASP code for different mixtures of fine mode (anthropogenic particles) and coarse mode (dust particles) revealed that F_{11} and $-F_{12}/F_{11}$ are sensitive to the different contribution of each mode in the mixture, being especially critical for $-F_{12}/F_{11}$ on the 405 nm channel. The negative values for $-F_{12}/F_{11}$ in 405 nm were observed more clearly for the mixture of fine and coarse particles. Thus, these simulations have served to understand the experimental negative values in $-F_{12}/F_{11}$ not observed in laboratory measurements for collected dust. Retrievals of bimodal size distribution with separate refractive indexes for each mode would have shown clarity to this problem. Hower, such retrieval with GRASP using F_{11} and $-F_{12}/F_{11}$ as inputs needs to be optimized. Another additional optimization in GRASP will imply the possibility of implementing the retrieval of super-coarse mode particles. The possibility of implementing

the irregular-hexahedral model would be also ideal to better understand polarization patterns. Nevertheless, the possibility of explaining the spectral differences in F_{11} and $-F_{12}/F_{11}$ with wavelength has served to understand the temporal evolution of the extreme dust events and the difference and similitudes when comparing versus laboratory measurements and versus other more moderate events of Saharan dust transport. However, going further in understanding the interaction of dust with these anthropogenic particles requires further analyses that provide the chemical composition and size distribution of the ensemble of particles. This is planned in future studies that will allow a more complete comprehensive analysis.

Additional comments*

There were some technical comments that we apologize for not addressing before. One was related to the inclusion of the "competing interest section". Now it is given between Lines 859-860

Competing interests

The authors declare that they have no conflict of interest.

Also, we were required to ensure that the colour schemes used in our maps and charts allow readers with colour vision deficiencies to correctly interpret your findings. We were not aware of this and we apologize for not following the guidelines We strongly support this way to make the manuscript more accessible to colour vision deficiencies people. We check Fig. 6, 7 and 8 using the Coblis – Color Blindness Simulator (https://www.color-blindness.com/coblis-color-blindness-simulator/) and revise the colour schemes accordingly.

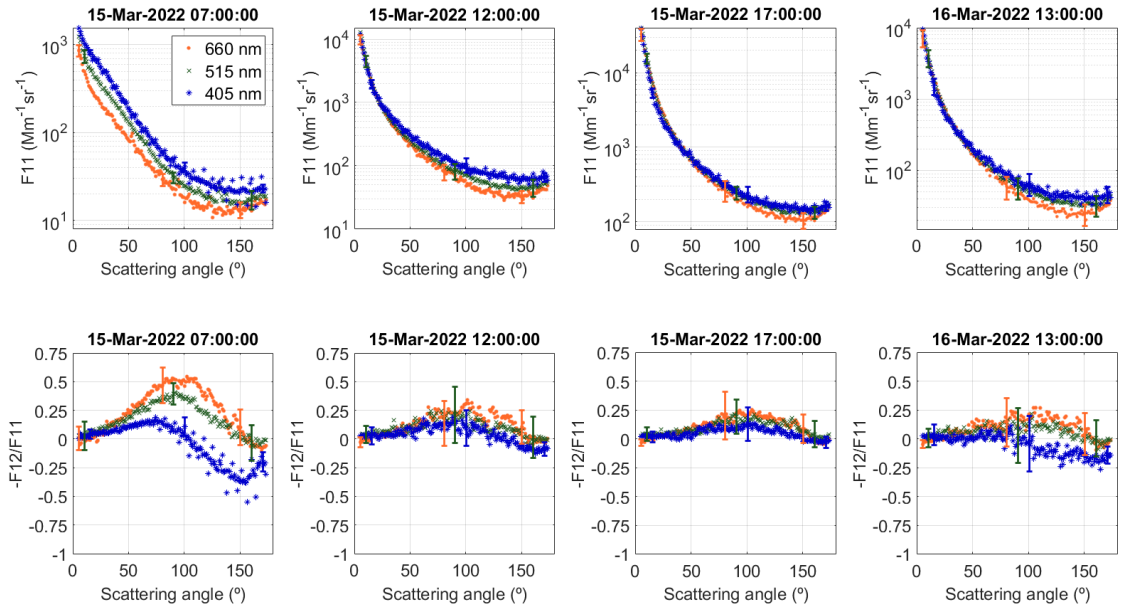

Figure 6. Hourly averages of phase function (F_{11}) and polarized phase function ($-F_{12}/F_{11}$) on 15th - 16th March 2022 for four different stages of the evolution of the extreme Saharan dust outbreak: (a) 15th March 07:00 UTC before the Saharan dust outbreak reached the station, (b) 15th March 12:00 UTC when the Saharan dust begins to reach the station, (c) 15th March 17:00 UTC associated with the peak of the extreme Saharan dust intrusion, and (d) 16th March 13:00 UTC when Saharan dust starts to withdrawn. Error bars correspond to the standard deviation of the hourly averages.

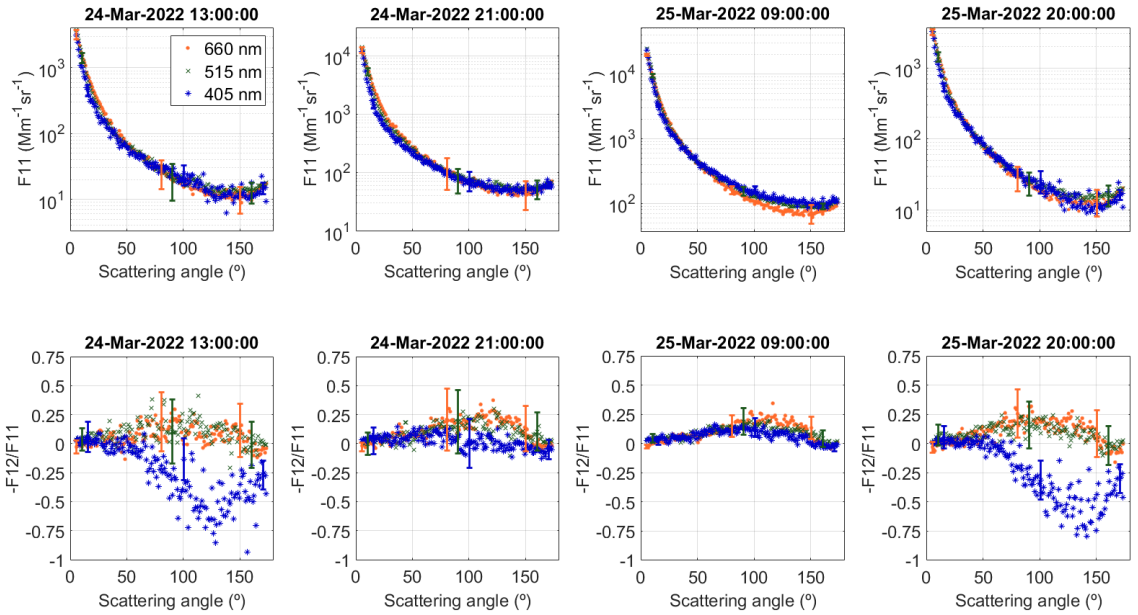

Figure 7. Hourly averages of phase function (F_{11}) and polarized phase function ($-F_{12}/F_{11}$) on 24th - 25th March 2022 for four different stages of the evolution of the extreme Saharan dust outbreak: (a) 24th March 13:00 UTC before the Saharan dust outbreak reached the station, (b) 24th March 21:00 UTC when the Saharan dust starts to reach the station, (c) 25th March 09:00 UTC associated with the peak of the extreme Saharan dust outbreak, and 25th March 20:00 UTC when dust begins to withdrawn. Error bars correspond to the standard deviation of the hourly averages.

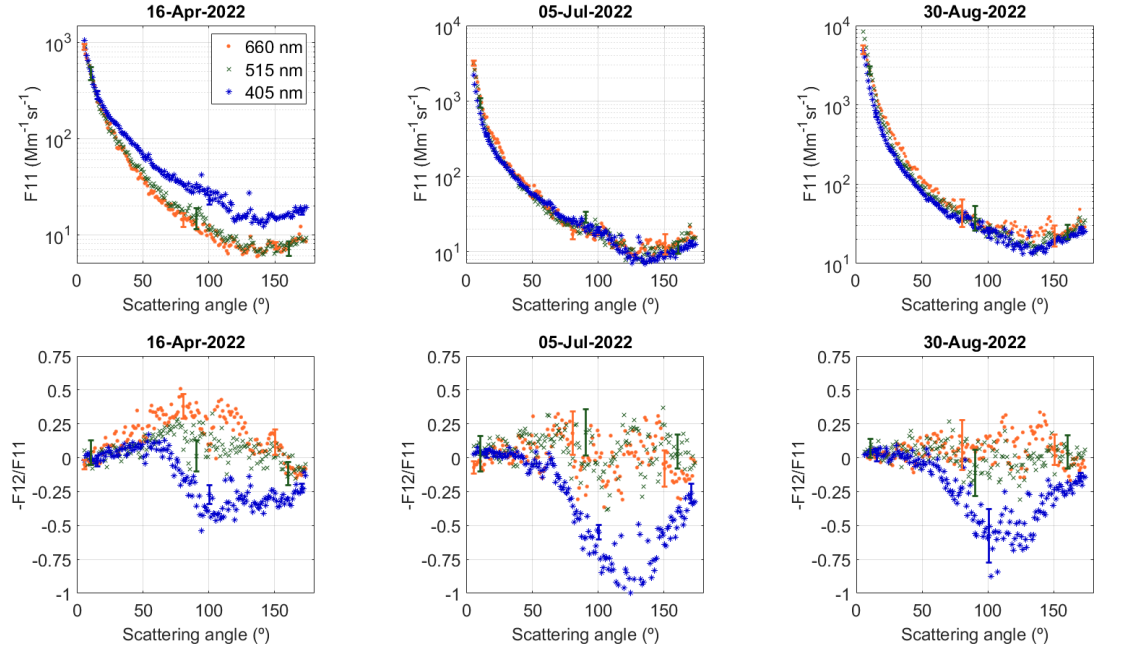

Figure 9. Phase function (F_{11}) and polarized phase function ($-F_{12}/F_{11}$) (for different moderate dust events: 15th April 202, 25th July 2022 and 30th August 2022. Error bars correspond to the standard deviation of the hourly averages.